Title: Range expansion is both slower and less predictable across a spatial gradient in temperature

Authors: Takuji Usui[1], Amy L. Angert[1,2]

Author affiliations:
[1]Department of Botany, University of British Columbia, Vancouver, British Columbia, V6T 1Z4, Canada (usuitakuji@gmail.com)
[2]Department of Zoology, University of British Columbia, Vancouver, British Columbia, V6T 1Z4, Canada (angert@mail.ubc.ca)

Corresponding author: Takuji Usui (Department of Botany, University of British Columbia, 2122 Main Mall, Vancouver, BC, V6T 1Z4, Canada; email: usuitakuji@gmail.com)

Running title: Range expansion across abiotic gradients

Keywords: biological invasion; demography; dispersal; eco-evolutionary dynamics; environmental gradient; experimental evolution; priority effects; range limit; variability

Article type: Letter
Word counts: Abstract (149), Main text (4989)
Number of references: 52
Number of figures: 4

Statement of authorship: TU conceived of this study with guidance from ALA. TU collected the data. TU analysed the data, developed the figures, and wrote the first draft of the manuscript with feedback from ALA. TU and ALA contributed to edits in preparation for manuscript submission.

Data accessibility statement: Data and R codes used for analyses are available on Zenodo: https://doi.org/10.5281/zenodo.8352240

ABSTRACT

Rapid evolution in colonizing populations can alter our ability to predict future range expansions. Recent studies suggest that how evolution influences the predictability of range expansion speed depends on the balance of genetic drift and selection at the range front, with factors increasing selection proposed to produce greater consistency, and hence increased predictability, in range expansion speed. Here, we test whether selection from environmental gradients across space produces more predictable range expansion speeds, using the experimental evolution of replicate, duckweed populations colonizing landscapes with and without a temperature gradient. While range expansion across a temperature gradient was slower, with range-front populations displaying higher population densities and genetic signatures consistent with greater selection, we found that range expansion speed was more variable and less predictable across replicate populations. Our results therefore challenge current theory, highlighting that selection and spatial priority effects could together govern the predictability of range expansion speeds.

INTRODUCTION

Predicting the movement of species ranges is a fundamental goal of ecology and is of increasing importance as biological invasions and climate change accelerate range expansion (Chen et al. 2011; Iseli et al. 2023; Nadeau & Urban 2019). Classic work on the ecological dynamics of range expansion has demonstrated that higher values of two key life-history traits – dispersal and reproductive output – increase the speed of range expansion (Kot et al. 1996; Skellam 1951). More recent work incorporating rapid evolution has shown that not only can dispersal and reproduction evolve to increase the average speed of range expansion, but that additionally,

evolution can directly influence the amount of variability in the speed of population spread across replicate, range-expanding populations (Miller et al. 2020; Ochocki & Miller 2017; Williams et al. 2016; Wiliams et al. 2019). However, when and in what direction evolution modifies the variability, and hence predictability, of range expansion remains unclear.

On one hand, eco-evolutionary studies of range expansion predict that evolution should increase variability in range expansion speed across replicate populations. Specifically, serial founding events during range expansion can result in the fixation of maladaptive alleles at the range front and consequent reduction in fitness (‘expansion load’) through a spatial analogue of genetic drift (‘gene surfing’) (Excoffier et al. 2009; Klopfstein et al. 2006; Perrier et al. 2020). Gene surfing in small, range-expanding populations leads to the fixation of random amounts of expansion load across replicate populations, thus generating variability in range expansion speed (Miller et al. 2020; Phillips 2015; Williams et al. 2019). The implication then, is that any single realisation of range expansion in nature is drawn from a distribution of possible outcomes, making predictions of range expansion more difficult.

In contrast, some recent experimental work testing the predictability of range expansions shows that evolution can also reduce variance in range expansion speed (Miller et al. 2020; Williams et al. 2019). This is predicted to occur when directional selection (e.g., for traits conferring greater dispersal or environmental tolerance; Chuang & Peterson 2016; Freedman et al. 2020; Lancaster et al. 2015) reduces trait variance at the range front, hence increasing consistency in the average speed of range expansion (Phillips 2015; Williams et al. 2019). Overall, how evolution modifies the variability in range expansion speed may therefore depend on the relative strength of gene

surfing and selection in range-front populations, and the factors that tip this balance one way or another (Miller et al. 2020; Urquhart-Cronish et al. 2022; Williams et al. 2019).

One key factor that could tip this balance between the variance-generating and variance-reducing effects of evolution is environmental variation in space. Specifically, species' ranges in nature exist across broad-scale spatial abiotic gradients. Importantly, changing abiotic conditions across space could lead to slower range expansion due to the need for populations to adapt to the underlying abiotic gradient. This initial maladaptation at the range front can allow more time for individuals to arrive from the range core, consequently increasing population size and genetic variation at the range front over time (Fronhofer et al. 2017; Gilbert et al. 2017). In these 'steeper' range boundaries, directional selection favouring traits that confer tolerance to changing abiotic conditions could weaken gene surfing and its genetic and demographic consequences (Gilbert et al. 2017; Williams et al. 2019). Thus, selection from underlying abiotic gradients in space could make the speed of range expansion among replicate populations less variable and more predictable. Although there is a need to incorporate realistic sources of environmental variation, experimentally testing how selection from abiotic gradients in space modifies the predictability of replicate range expansions in nature remains difficult (Miller et al. 2020).

Experimental range expansions in "miniaturised" landscapes (Larsen & Hargreaves 2020; Lustenhower et al. 2023) can provide a powerful bridge between theory and range expansion in natural landscapes. First, these landscapes differ from traditional microcosms in that replicate populations can disperse naturally across linear landscapes, such that realistic genetic and demographic spatial structure arises during range expansions. Second, through replicated

100 landscapes we can track a distribution of ecological and evolutionary outcomes in colonising
101 populations. This allows experimental insights into the factors that contribute to variability in
102 range expansion that would not be possible without replication. Third, through experimental
103 evolution we can track the eco-evolutionary dynamics of range expansion unfolding over
104 multiple generations in real time, while field studies have mostly been retrospective, inferring
105 past demographic and evolutionary processes based on current spatial patterns. Despite the
106 increasing utility of these landscapes (Larsen & Hargreaves 2020), we still require experiments
107 that test the dynamics of range expansion across landscapes that incorporate selection from
108 spatial environmental variation.
109
110 Here, we use experimental populations of duckweeds in the *Lemna* species complex to
111 experimentally test how selection from spatial abiotic gradients modifies the predictability (i.e.,
112 among-replicate variability) of range expansion speed. Using replicate landscapes with and
113 without a temperature gradient in space, we predicted that: (i) range expansion speed should be
114 more predictable (i.e., less variable among replicates) when populations move across landscapes
115 with a spatial temperature gradient than without. We predicted that this would occur as: (ii) range
116 expansion across temperature gradients would be on average slower, resulting in higher
117 population densities and steeper range boundaries. Consequently, we predicted that there should
118 be stronger signatures of selection over genetic drift in populations expanding across temperature
119 gradients. If selection was stronger in populations expanding across temperature gradients in
120 space, then we predict: (iii) less among-replicate variability in genotypic composition for
121 gradient than uniform landscapes; and (iv) directional selection for traits relevant to thermal
122 tolerance in these populations.

123

124 **MATERIALS & METHODS**

125 ***Lemna* species collection and culturing**

126 Duckweeds are small, freshwater angiosperms with a rapid generation time of 2–5 days under
127 ideal conditions (Landolt 1986). Although sexual reproduction occurs sporadically in nature,
128 reproduction during experiments occurs exclusively through the clonal budding of daughter
129 fronds (Docauer 1983; Landolt 1986). Multiple fronds can stay connected via a stipule to form
130 rafts of ~3-5 fronds until the stipule breaks and daughter fronds disperse. We sampled 20 unique
131 accessions of duckweeds in the *Lemna* species complex from 20 sites around the Pacific
132 Northwest region of North America (Table S1). Upon sampling, we immersed fronds in a dilute
133 bleach solution (10% v:v) to create axenic plants of each accession. We maintained each of our
134 20 accessions in 250 mL erlenmeyer flasks with 100 mL of artificial pond media (Appenroth et
135 al. 1996), inside a temperature-controlled laboratory (20°C) and under full-spectrum LED
136 lighting (SunBlaster 6400K; 16:8 hour light:dark cycle). To obtain sufficient numbers of
137 individuals for the experiment, we grew out each accession for 4 weeks inside 20 L buckets at
138 the UBC Botany greenhouse, with 17 L of water, 4 L of autoclaved potting soil (MiracleGro
139 Potting Mix), 1.32 mM of KNO_3, 0.16 mM of $Ca(NO_3)_2$, and 0.02 mM of KH_2PO_4 as fertilisers.

140

141 Duckweeds in the *Lemna* species complex are thought to be comprised of *L. minor*, *L.*
142 *turionifera*, and *L. japonica*. These three lineages are ecologically and genetically cryptic, and
143 species delineation is currently a challenge despite the development of various molecular
144 markers (Braglia et al. 2021a; Braglia et al. 2021b). Our barcoding approach based on Tubulin-
145 Based Polymorphism (TBP) fingerprinting (Braglia et al. 2021a) and microsatellite genotyping

146 of each accession detected that our accessions were composed of 6 unique genotypes of *L. minor*
147 and 5 genotypes of *L. japonica* (Appendix S1; Tables S1-S3). While some studies have proposed
148 that *L. japonica* is a hybrid between *L. minor* and *L. turionifera* (Braglia et al. 2021a; Braglia et
149 al. 2021b; Volkova et al. 2023), we note that taxonomic delineation between these groups is at
150 present unstable. In our experiment, we therefore describe evolution as occurring through the
151 sorting of unique genotypes within the *Lemna* species complex.
152
153 **Experimental landscapes and temperature treatment**
154 We set up 50 experimental landscapes across five benches inside the greenhouse, with each
155 landscape constructed from aluminium gutters (150 cm x 12.5 cm; L x W) and filled with 13.5 L
156 of water and 2.5 L of potting soil. To ensure nutrients and water-levels did not deplete over time,
157 we added 0.13 mM of KNO_3, 0.02 mM of $Ca(NO_3)_2$, and 0.002 mM of KH_2PO_4 every 4 days to
158 each landscape, and continuously regulated water-levels using a float-valve connected to a sump
159 pump. We connected drip emitters to the sump pump so that water refilling occurred slowly and
160 did not disrupt the spatial structure of populations. We set up a temperature treatment (Fig. 1a)
161 such that range expansion occurred across landscapes with a spatial gradient in temperature
162 ("gradient landscapes" hereafter; $N = 25$) or with spatially uniform temperatures ("uniform
163 landscapes" hereafter; $N = 25$). The position of gradient and uniform landscapes was randomised
164 within each bench. To establish a temperature gradient, we used a submersible heater (150W JBJ
165 aquarium heaters) set to 37°C and placed at one end of each gradient landscape. To maintain
166 uniform temperatures, we placed two heaters set to 24°C at both ends of each uniform landscape.
167 These set temperatures were chosen as they are close to the critical thermal maxima (T_{max}) and
168 thermal optima (T_{opt}), respectively, of the *Lemna* genotypes used (Fig. S1). We monitored water

169 temperatures using three underwater temperature loggers (HOBO pendants) placed at equal
170 spacing within each landscape. For gradient and uniform landscapes, the imposed temperature
171 treatment resulted in increasing or uniform temperatures across space, respectively (Fig. 1b).
172 Although our initial aim for gradient landscapes was to set up a stress gradient such that
173 populations experienced increasing heat stress as they dispersed, we note that: (i) average
174 temperatures at the experimental range limit of gradient landscapes were still relatively benign
175 (31.6°C; SD = 1.9°C; Fig. 1b); and (ii) as average temperatures across space were similar
176 between gradient and uniform landscapes (27.4°C; SD = 3.85°C and 26.9°C; SD = 1.53°C,
177 respectively), temperatures at the start of gradient landscapes were relatively cooler than in
178 uniform landscapes (24.3°C; SD = 2.6°C and 27.6°C; SD = 1.4°C, respectively). However, we
179 note that our temperature treatment still reflects the presence and absence of a temperature
180 gradient across space in gradient and uniform landscapes, respectively.
181
182 **Range expansion**
183 To initiate range expansion, we established genetically diverse *Lemna* populations, with each
184 population consisting of an even density of 20 accessions (N = 20 individuals per accession for a
185 founding population size of N = 400 individuals). We seeded each population at one end of each
186 landscape, allowing 2 days for plants to acclimate before range expansion. In gradient
187 landscapes, we seeded populations at the cooler end of the landscape and allowed range
188 expansion into increasingly warmer temperatures (Fig. 1a). To allow all populations the
189 opportunity to colonize the full spatial extent of the landscape, the experiment ran for 112 days.
190 During our experiment, we lost one replicate due to structural damage and lost 10 replicates on
191 one bench due to a disturbance event that disrupted population spread. We also lost 6 replicates

192 due to heavy algal growth on the water surface that obstructed population spread. In total, we
193 retained 33 experimental landscapes across four benches (*N* = 16 gradient landscapes; *N* = 17
194 uniform landscapes).
195
196 **Quantifying range expansion speed**
197 We quantified the mean and variability in range expansion speed across landscapes for the initial
198 24 days (i.e., ~5–12 generations) of range expansion. This timescale represents population spread
199 during the exponential growth phase and thus is most consistent with theoretical models of range
200 expansion (Kot et al. 1996; Skellam 1951). Also, some populations had reached the range limit
201 of landscapes by day 24. These replicates would not be able to spread further and their inclusion
202 after 24 days would artificially reduce the average and among-replicate variability in range
203 expansion speed (i.e., the ceiling effect).
204
205 To quantify range expansion speed, we took aerial photographs of each landscape every 4 days
206 (Nikkon D750; AF-S Nikkor 24-120 mm f/4G ED VR). From these images, we first quantified
207 the maximum distance travelled (cm) for each population by measuring the distance reached by
208 the furthest individual every 4 days. We then quantified the mean and among-replicate variability
209 in the distance travelled at each treatment level and time point. To estimate the difference in
210 among-replicate variability of distance travelled for gradient and uniform landscapes, we
211 calculated the log coefficient of variation ratio (lnCVR; Nakagawa et al. 2015) as:
212 $$lnCVR = \frac{lnCV_E}{lnCV_C} + \frac{1}{2(n_E-1)} - \frac{1}{2(n_C-1)} \qquad (1)$$

where subscripts *E* and *C* refer to the experimental (i.e., gradient) and control (i.e., uniform) landscapes, CV is the coefficient of variation, and *n* is the sample size. We calculated lnCVR such that positive values correspond to larger variability in distance travelled among gradient compared to uniform landscapes. We use lnCVR because CV accounts for the linear and positive mean-variance relationship on the log scale (Fig. S2; Taylor 1961). To report differences in CV, we back-transformed estimates of lnCVR.

Quantifying range-front population density and steepness

We quantified spatiotemporal changes in population density at the range front by estimating the percent cover of live (i.e., green) fronds on the water surface. We did this by colour thresholding images obtained every 4 days using ImageJ (v1.53) and estimating percent cover in 2 cm x 12.5 cm grids at the range front (defined as the first 12 cm from the furthest travelled individual). We then fit a logistic model of percent cover across space for each landscape to quantify the maximum population density at the range front at each time point. We also quantified the steepness of the range boundary (i.e., the rate of increase in population density) by fitting an exponential model to the first three estimates of percent cover at the range front of each landscape. Steepness was quantified as the exponent obtained from each model (Legault et al. 2020).

Quantifying range-front evolution

We quantified evolution as the change in genotype frequencies due to genotype sorting from the founding population. Post-experiment, we haphazardly sampled 12 individual rafts of duckweeds from each replicate range front. Each sample was then genotyped using four microsatellite

236 markers in a single multiplex reaction (Appendix S1; Table S2; Hart et al. 2017). We
237 successfully obtained genotype sequences for 272 individuals (88% of all genotyped samples).
238 To balance the number of samples obtained within each replicate and treatment, we rarefied
239 samples and dropped replicates represented by less than $N = 6$ individuals due to DNA extraction
240 or genotyping failure. For all downstream analyses, we therefore obtained a total of $N = 6$
241 individuals per replicate, for 10 and 17 replicates of gradient and uniform landscapes,
242 respectively. We note a higher extraction and genotyping failure for samples obtained from
243 gradient landscapes possibly due to greater damage to plant tissue from heat stress.
244
245 To investigate whether genotype sorting in the experiment led to consistent trait evolution, we
246 also measured a suite of genotype-specific traits *ex situ* in incubators and across a range of
247 temperatures (Appendix S2; Fig. S1). We parameterized traits hypothesised to be ecologically
248 relevant to range expansion across thermally variable landscapes, including: maximum growth
249 rate (r_{max}); thermal optimum (T_{opt}); critical thermal maximum (CT_{max}); critical thermal minimum
250 (CT_{min}); thermal breadth (i.e., the range of temperatures for which growth rate is within 80% of
251 the maximum; Padfield et al. 2021); thermal tolerance (i.e., the difference between CT_{max} and
252 CT_{min}); mean specific-leaf area (SLA; cm^2/g); mean root-shoot ratio (cm/mg); and plasticity in
253 both SLA and root-shoot ratio, as quantified by its CV across temperature (see Table S10 for
254 trait estimates at the genotype level). Before analyses, we scaled and centred each trait, and
255 estimated mean trait values at the population level for both our founding and evolved populations
256 by weighting trait values by the observed genotype frequencies of each population.
257
258 **Statistical analyses**

We tested whether temperature treatment led to differences in the ecological dynamics of range expansion. First, we tested for treatment differences in mean range expansion speed by fitting a linear mixed-effects model using the *lme4* package (Bates et al. 2015). We fit maximum distance travelled (cm) as the response variable and an interaction between time (day) and temperature treatment (gradient *vs* uniform) as fixed predictors, where mean range expansion speed is modelled as slopes (cm/day). We also included bench ID as a fixed covariate and fitted a random slope (i.e., speed) for each replicate. Second, we tested for treatment differences in among-replicate variability of distance travelled by fitting a linear model with lnCVR as the response variable and time as the predictor. We modelled the temporal trend in lnCVR as visual inspections of CV in distance travelled showed changes over time for both gradient and uniform landscapes (Fig. 2b). For sensitivity analyses, we also conducted a linear meta-regression of lnCVR to explicitly model the sampling variation around each observation (Appendix S3). Third, we tested for treatment differences in range-front population density (i.e., carrying capacity) and steepness of the range boundary (i.e., exponent) by fitting separate linear regressions with either population density or steepness as the response variable, respectively, and time, temperature treatment, and their interaction as predictors. For sensitivity analyses, we also conducted a separate meta-regression of population density and steepness by including the standard error around each observation using the package *metafor* (Viechtbauer 2010).

We also tested whether temperature treatment led to differences in the evolutionary dynamics of range expansion. First, we tested for treatment differences in the amount of genotypic or trait change, as estimated by the Euclidean distance between the initial genotype or trait frequency in the founding population and the post-experimental genotype or trait frequency for each

282 landscape. We fit separate linear regressions with Euclidean distance of genotype or trait
283 frequencies as the response variable, temperature treatment as the predictor, and bench ID as a
284 fixed covariate. Second, we tested for treatment differences in the final genotype or trait
285 composition in range-front populations. Here, we quantified compositional dissimilarity of
286 genotypes or traits across all pairwise populations within each treatment using Euclidean
287 dissimilarity matrices. We then conducted separate PERMANOVAs using *adonis2* in the *vegan*
288 package (Okansen et al. 2022) with genotype or trait dissimilarity among replicates as the
289 response variable, temperature treatment as the predictor, and bench ID as a fixed covariate.
290 Upon observing differences in genotype composition, we tested whether certain genotypes arose
291 to higher frequencies than predicted by chance by conducting a post-hoc binomial test on the
292 mean frequency of each genotype for each temperature treatment. Third, we tested whether
293 temperature treatment led to differences in the amount of among-replicate variability found in
294 the genotype composition of range-front populations. To quantify the amount of observed
295 among-replicate variability, we first averaged genotype frequencies across replicates within each
296 treatment. For each temperature treatment, we then calculated the Euclidean distance between
297 this mean genotype composition and the observed genotype composition of each replicate. As a
298 measure of the observed among-replicate variability in genotype composition, we then summed
299 these Euclidean distances across all replicates within each treatment. We tested for treatment
300 differences in among-replicate variability through a permutation test, with Euclidian distances
301 permuted randomly across treatment 100,000 times. Finally, we tested whether the observed
302 among-replicate variability in each treatment differed from that predicted by random sampling.
303 To quantify among-replicate variability predicted by random sampling, we first pooled
304 genotypes across replicates within each temperature treatment. From this pool, we randomly

305 drew 6 individuals with replacement (i.e., representing the 6 genotypes in our observed data) and
306 repeated this *N* times for each treatment, where *N* is the number of replicates for gradient (*N* =
307 10) and uniform landscapes (*N* = 17). We then estimated the mean genotype composition for
308 each temperature treatment and calculated the Euclidean distance between the simulated mean
309 genotype composition and the simulated genotype composition of each replicate. We summed
310 these Euclidean distances for each treatment as a measure of the among-replicate variability in
311 genotype composition predicted by random sampling. We repeated this simulation a total of
312 100,000 times to estimate the probability of obtaining the observed among-replicate variability in
313 genotype composition for each treatment based on random sampling. All model-fitting was
314 conducted in R (R Core Team 2020).
315

316 **RESULTS**

317 **Temperature treatment on range expansion speed**

318 On average, we found that range expansion speed across gradient landscapes was slower than
319 across uniform landscapes (time by treatment effect: $P = 0.016$; Table S4; Fig. 2a), consistent
320 with prediction (ii). Over 24 days of range expansion, the presence of a spatial temperature
321 gradient reduced the average speed of range expansion by 50.9% (95% CI: 36.0% to 53.8%)
322 compared to uniform landscapes (Table S4). We also found that the among-replicate variability
323 in distance travelled differed between gradient and uniform landscapes (Fig. 2b and 2c). At the
324 initial stages of range expansion, we found that there was less among-replicate variability (CV)
325 in distance travelled across gradient compared to uniform landscapes (e.g., a 40.3% [95% CI:
326 28.6% to 56.8%] reduction in CV across gradient compared to uniform landscapes on day 4;
327 Table S5), consistent with prediction (i). However, we found a significant increase in lnCVR

328 over time (lnCVR slope: $P = 0.002$) such that by day 24, CV in distance travelled was 78.2%
329 (95% CI: 28.6% to 151.0%) greater across gradient than uniform landscapes (Fig. 2c), contrary
330 to prediction. This result was consistent when including sampling variation around lnCVR in the
331 linear model (Table S5).
332
333 **Temperature treatment on range-front density and steepness**
334 We found that the population density reached at the range front differed over time and between
335 gradient and uniform landscapes (Fig. 2d-f). Although range-front densities were initially similar
336 between gradient and uniform landscapes, population density increased more rapidly over time
337 for gradient landscapes (treatment by time effect: $P = 0.002$; Fig. 2f), consistent with prediction
338 (ii). By day 24, population density at the range front was 88.1% (95% CI: 76.5% to 104.0%)
339 higher in gradient compared to uniform landscapes (Table S6). Along with increased population
340 density, we also found range boundaries to be steeper in gradient landscapes (Table S7; Figure
341 S3), consistent with prediction (ii). These results were consistent in sensitivity models that
342 included sampling error in estimates of range-front population density and steepness (Tables S6
343 and S7).
344
345 **Temperature treatment on evolutionary change**
346 We found that evolution in range-front populations (i.e., change in genotype frequencies from
347 the founder population) occurred in both gradient and uniform landscapes (Intercept: $P < 0.001$;
348 Table S8). We found partial support for prediction (iii) that selection is greater in gradient
349 landscapes. On average, the observed among-replicate variability in genotype composition was
350 greater in uniform compared to gradient landscapes (Fig. 4), although permutation tests revealed

351 that this treatment difference was non-significant ($P = 0.304$). Importantly, we found that the
352 observed among-replicate variability in genotype composition was greater than predicted by
353 random sampling for both gradient ($P = 0.003$) and uniform ($P < 0.001$) landscapes (Fig. 4). We
354 also found that genotype composition of range-front populations differed between gradient and
355 uniform landscapes after range expansion (PERMANOVA: $P = 0.002$; Table S9; Fig. 3a).
356 Specifically, range-front populations in gradient landscapes were often dominated by one
357 genotype (G11; Fig. 3c), with post-hoc binomial tests showing that this genotype consistently
358 increased in frequency in gradient landscapes ($P < 0.001$) but not in uniform landscapes ($P =$
359 0.869), suggesting selection for this genotype in the former (Fig. 3e).
360
361 Trait evolution (i.e., change in trait frequencies from the founder population) occurred in both
362 gradient and uniform landscapes (Intercept: $P = 0.004$; Table S8; Fig. S4). However, contrary to
363 prediction (iv), out of the 11 traits assessed we did not find significant treatment differences in
364 the extent of trait change (Treatment effect: $P = 0.345$; Table S8) or in trait composition of
365 range-front populations (PERMANOVA: $P = 0.088$; Table S9; Fig. S4).
366
367 **DISCUSSION**
368 Recent studies have highlighted that rapid evolution can complicate our ability to predict the eco-
369 evolutionary dynamics of range expansions (Miller et al. 2020; Shaw et al. 2023; Williams et al.
370 2019; Zilio et al. 2023). Here, we used replicate range-expanding populations to empirically test
371 whether the presence of selection from an abiotic gradient across landscapes could modify the
372 among-replicate variability, and hence predictability, of range expansion speed. Notably, we
373 found that over time range expansion speed became more variable, and hence less predictable, in

374 landscapes with a spatial temperature gradient than without (Fig. 2c). This occurred despite
375 gradient landscapes having slower range expansions on average, greater range-front population
376 densities (Fig. 2), and genetic signatures consistent with increased selection (Fig. 3)– conditions
377 that would otherwise predict less gene surfing and thus more consistency in the speed of range
378 expansions across replicate populations (Miller et al. 2020; Phillips 2015; Williams et al. 2019).
379 Our results therefore challenge current theory and highlight the complexities of predicting range
380 expansions even in highly standardised, replicate mesocosms with simple environmental
381 variation.
382
383 We found that the greater variability in range expansion speed observed for gradient compared to
384 uniform landscapes over time is driven by a combination of rapidly decreasing among-replicate
385 variability (CV) in distance travelled for uniform landscapes, and slightly increasing CV for
386 gradient landscapes over time (Fig. 2b). In uniform landscapes, the decrease in CV of distance
387 travelled over time occurred as mean range expansion speed increased more quickly than the
388 variance observed across replicates (Fig. 2a). A rapid increase in mean range expansion speed
389 across uniform landscapes is consistent with previous experimental evolution work on range
390 expansions, which found that range expansion speed can increase under constant environments
391 due to spatial sorting for dispersal phenotypes and low-density selection for increased
392 reproductive output at the range front (Ochocki & Miller 2017; Wagner et al. 2017; Weiss-
393 Lehman et al. 2017). In contrast, for gradient landscapes, the slight increase in CV of distance
394 travelled over time occurred as the variance in speed among replicates increased more quickly
395 than the mean range expansion speed (Fig. 2a). This occurred as range expansion remained slow

396 for most gradient landscapes but rapidly sped up in a few replicates (Fig. 2a), consequently
397 elevating the among-replicate variability observed over time.
398
399 It is possible that the faster range expansion seen in some of these gradient landscapes was partly
400 driven by selection from the temperature gradient (Moerman et al. 2022; Phillips et al. 2006;
401 Szücs et al 2017; Williams et al. 2016). We found that gradient landscapes had consistently
402 higher frequencies of one genotype (G11) at the range front (Fig. 3c and 3d). In contrast, this
403 genotype did not achieve frequencies >0.5 in any range-front population for uniform landscapes
404 (Fig. S5). We note that the evolutionary dynamics described above reflect longer term range
405 expansion and selection after 112 days (~22-56 generations), while the population dynamics
406 reflect shorter term range expansion in the first 24 days (~4-12 generations). Even so,
407 comparison to genetic data obtained at an earlier point in time from the fastest range-expanding
408 replicates confirm that this same genotype had reached high frequencies at the range-front of
409 gradient landscapes but not in uniform landscapes (Fig. S6), suggesting that rapid evolution in
410 the former occurred as early as within the first 36 days (i.e., 7–18 generations) of range
411 expansion.
412
413 While we did not find trait composition to differ significantly between gradient and uniform
414 landscapes within the 11-dimensional trait space (Fig. S4), post-hoc comparison of univariate
415 trait means revealed that this high-frequency genotype in gradient landscapes has both the
416 highest mean estimate of thermal breadth and the lowest maximum growth rates among all
417 genotypes (Table S10). The importance of maintaining performance across a broader range of
418 temperatures through thermal breadth evolution has been long emphasised in studies of range

419 expansion across latitudinal gradients in climate (Ackerly 2003; Lancaster 2016; Lancaster 2022)
420 and is also consistent with studies that report a positive relationship between range size and niche
421 breadth (Slatyer et al. 2013). While it could be surprising that range-expanding populations are
422 also fixed for the genotype with the lowest maximum growth rate, this could be explained by
423 generalist-specialist trade-offs between sustaining growth rates across a wider range of
424 temperatures and obtaining high growth rates at the temperature optimum (Huey & Hertz 1984).
425 Additionally, models of range expansion that incorporate density-dependence and life-history
426 trade-offs also predict that higher population densities and steeper range boundaries, as observed
427 in our gradient landscapes, can favour *K*-selected traits (e.g., increased competitive ability) at the
428 range front even if this comes at a cost of *r*-selected traits (e.g., increased reproductive output
429 and growth rates; Burton et al. 2010; Pachepsky & Levine 2011; Williams et al. 2016).
430
431 However, while the consistently high frequency of this genotype suggest that selection was
432 stronger at the range front of gradient over uniform landscapes, we also found in both landscapes
433 that the among-replicate variability in genetic composition was greater than predicted by random
434 sampling (Fig. 4). Such a pattern could result if the eco-evolutionary dynamics of range
435 expansion in landscapes with environmental variation is governed by a combination of selection
436 and spatial priority effects, such that the genotypes available to respond to selection in range-
437 front populations is shaped by individuals that initially occupy the range front through chance
438 dispersal (Baym et al. 2016; Hallatschek et al. 2007; Hewitt 2000; Williams et al. 2016). Taken
439 together, we propose that spatial priority effects and its variance-generating effects at the range
440 front, combined with directional selection from abiotic gradients in space, could lead on average

441 to slower but more variable speeds during range expansion, relative to range expansion across
442 uniform environments.
443
444 Our results highlight that even in ecological conditions under which the effects of gene surfing
445 are reduced, the speed of range expansion can be variable and difficult to predict. Previous
446 experimental and theoretical work suggest the predictability of range expansion speed depends
447 on the balance of evolutionary processes that generate and reduce variability (i.e., gene surfing
448 and selection, respectively) and the ecological factors that tip this balance (Miller et al. 2020;
449 Williams et al. 2019). We additionally suggest that predicting the dynamics of range expansion
450 may require an understanding of how selection interacts with spatial priority effects, and whether
451 priority effects could hamper the response to selection and increase among-replicate variability
452 in the speed of range expansion. As populations traverse across environmentally variable and
453 complex landscapes, studies of natural range expansions will need to incorporate how selection
454 from underlying environmental variation in space can influence our ability to predict future
455 range expansions.
456
457 **ACKNOWLEDGEMENTS**
458 We thank H. Ahmed, M. Catalani, A. Doherty, K. Kubeck, E. Menchions, T. Scriber, and P.
459 Seppala for their help with plant and greenhouse maintenance, and for providing assistance with
460 experimental setup. We thank M. Chen, E. Lam, D. Moxley and A. Wong for their generous
461 assistance with genetic work. We are grateful to R. Germain, S. Otto, M. Tseng, and J. Williams
462 for their comments on earlier versions of the manuscript. This work was supported by the UBC

International Doctoral Fellowship and the SSE Greg Lewontin Award to TU, and a Discovery Grant from the Natural Sciences and Engineering Research Council of Canada to ALA.

REFERENCES

Ackerly, D.D. (2003). Community assembly, niche conservatism, and adaptive evolution in changing environments. *Int. J. Plant Sci.*, 164, S165–S184.

Appenroth, K.J., Teller, S. & Horn, M. (1996). Photophysiology of turion formation and germination in *Spirodela polyrhiza*. *Biol. Plantarum*, 38, 343–351.

Bates, D., Mächler, M., Bolker, B. & Walker, S. (2015). Fitting linear mixed-effects models using lme4. *J. Stat. Softw.*, 67, 1–48.

Baym, M., Lieberman T.D., Kelsic, E.D., Remy, C., Gross, R., Yelin, I. & Kishony, R. (2016). Spatiotemporal microbial evolution on antibiotic landscapes. *Science*, 353, 1147–1151.

Braglia, L., Breviario, D., Gianì, S., Gavazzi, F., De Gregori, J. & Morello, L. (2021a). New insights into interspecific hybridization in *Lemna* L. Sect. *Lemna* (Lemnaceae Martinov). *Plants*, 10, 2767.

Braglia, L., Lauria, M., Appenroth, K.J., Bog, M., Breviario, D., Grasso, A., *et al*. (2021b). Duckweed species genotyping and interspecific hybrid discovery by Tubulin-Based Polymorphism Fingerprinting. *Front. Plant. Sci.*, 12, 625670.

Burton, O.J., Phillips, B.L. & Travis, J.M.J. (2010). Trade-offs and the evolution of life-histories during range expansion: Evolution during range expansion. *Ecol. Lett.*, 13, 1210–1220.

Chen, I.C., Hill, J.K., Ohlemüller, R., Roy, D.B. & Thomas, C.D. (2011). Rapid range shifts of species associated with high levels of climate warming. *Science*, 333, 1024–1026.

Chuang, A. & Peterson, C.R. (2016). Expanding population edges: Theories, traits, and trade-offs. *Glob. Change Biol.*, 22, 494–512.

Docauer, D. M. (1983). *A nutrient basis for the distribution of the Lemnaceae*. Dissertation. University of Michigan, Ann Arbor, Michigan, USA.

Excoffier, L., Foll, M. & Petit, R.J. (2009). Genetic consequences of range expansions. *Annu. Rev. Ecol. Evol. S.*, 40, 481–501.

Freedman, M.G., Dingle, H., Strauss, S.Y., & Ramírez, S.R. (2020). Two centuries of monarch butterfly collections reveal contrasting effects of range expansion and migration loss on wing traits. *Proc. Natl. Acad. Sci. U.S.A.*, 117, 28887–28893.

Fronhofer, E.A., Nitsche, N. & Altermatt, F. (2017). Information use shapes the dynamics of range expansions into environmental gradients. *Glob. Ecol. Biogeogr.,* 26, 400–411.

Gilbert, K.J., Sharp, N.P., Angert, A.L., Conte, G.L., Draghi, J.A., Guillaume, F., *et al.* (2017). Local adaptation interacts with expansion load during range expansion: Maladaptation reduces expansion load. *Am. Nat.*, 189, 368–380.

Hallatschek, O., Hersen, P., Ramanathan, S. & Nelson, D.R. (2007). Genetic drift at expanding frontiers promotes gene segregation. *Proc. Natl., Acad. Sci. U.S.A.*, 104, 19926–19930.

Hart, S.P., Turcotte, M.M. & Levine, J.M. (2019). Effects of rapid evolution on species coexistence. *Proc. Natl., Acad. Sci. U.S.A.*, 116, 2112–2117.

Hewitt, G. (2000). The genetic legacy of the Quaternary ice ages. *Nature*, 405, 907–913.

Huey, R.B. & Hertz, P.E. (1984). Is a Jack-of-All-Temperatures a Master of None? *Evol.,* 38, 441–444.

Iseli, E., Chisholm, C., Lenoir, J., Haider, S., Seipel, T., Barros, A., *et al.* (2023). Rapid upwards spread of non-native plants in mountains across continents. *Nat. Ecol. Evol.*, 7, 405–413.

Klopfstein, S., Currat, M. & Excoffier, L. (2006). The fate of mutations surfing on the wave of a range expansion. *Mol. Biol. Evol.*, 23, 482–490.

Kot, M., Lewis, M.A. & Van Den Driessche, P. (1996). Dispersal data and the spread of invading organisms. *Ecol.*, 77, 2027–2042.

Lancaster, L.T., Dudaniec, R.Y., Hansson, B. & Svensson, E.I. (2015). Latitudinal shift in thermal niche breadth results from thermal release during a climate-mediated range expansion. *J. Biogeogr.*, 42, 1953–1963.

Lancaster, L.T. (2016). Widespread range expansions shape latitudinal variation in insect thermal limits. *Nat. Clim. Change*, 6, 618–621.

Lancaster, L.T. (2022). On the macroecological significance of eco-evolutionary dynamics: The range shift–niche breadth hypothesis. *Philos. T. R. Soc. B.*, 377, 20210013.

Landolt, E. (1986). *Biosystematic investigations in the family of duckweeds, Lemnaceae: the family of Lemnaceae, a monographic study*. Volume 2: Morphology, karyology, ecology, geographic distribution, systematic position, nomenclature descriptions. Veroeffentlichungen des Geobotanischen Institutes der ETH, Stiftung Rubel, Zurich, Switzerland.

Larsen, C.D. & Hargreaves, A.L. (2020). Miniaturizing landscapes to understand species distributions. *Ecography*, 43, 1625–1638.

Legault, G., Bitters, M.E., Hastings, A. & Melbourne, B.A. (2020). Interspecific competition slows range expansion and shapes range boundaries. *Proc. Natl. Acad. Sci. U.S.A.*, 117, 26854–26860.

Lustenhouwer, N., Moerman, F., Altermatt, F., Bassar, R.D., Bocedi, G., Bonte, D., *et al.* (2023). Experimental evolution of dispersal: Unifying theory, experiments and natural systems. *J. Anim. Ecol.*, 92, 1113–1123.

Miller, T.E.X., Angert, A.L., Brown, C.D., Lee-Yaw, J.A., Lewis, M., Lutscher, F., *et al.* (2020). Eco-evolutionary dynamics of range expansion. *Ecol.*, 101. e03139.

Moerman, F., Fronhofer, E.A., Altermatt, F. & Wagner, A. (2022). Selection on growth rate and local adaptation drive genomic adaptation during experimental range expansions in the protist *Tetrahymena thermophila*. *J. Anim. Ecol.*, 91, 1088–1103.

Nadeau, C.P. & Urban, M.C. (2019). Eco-evolution on the edge during climate change. *Ecography*, ecog.04404.

Nakagawa, S., Poulin, R., Mengersen, K., Reinhold, K., Engqvist, L., Lagisz, M., *et al.* (2015). Meta-analysis of variation: Ecological and evolutionary applications and beyond. *Methods Ecol. Evol.*, 6, 143–152.

Ochocki, B.M. & Miller, T.E.X. (2017). Rapid evolution of dispersal ability makes biological invasions faster and more variable. *Nat. Commun.*, 8, 14315.

Oksanen, J., Simpson, G.L., Blanchet, F.G., Kindt, R., Legendre, P. & Minchin, P.R. (2022). Vegan: Community ecology package (v 2.6–2).

Pachepsky, E. & Levine, J.M. (2011). Density dependence slows invader spread in fragmented landscapes. *Am. Nat.*, 177, 18–28.

Padfield, D., O'Sullivan, H. & Pawar, S. (2021). rTPC and nls.multstart: A new pipeline to fit thermal performance curves in R. *Methods Ecol. Evol.*, 12, 1138–1143.

Perrier, A., Sánchez-Castro, D. & Willi, Y. (2020). Expressed mutational load increases toward the edge of a species' geographic range. *Evol.*, 74, 1711–1723.

Phillips, B.L. (2015). Evolutionary processes make invasion speed difficult to predict. *Biol. Invasions*, 17, 1949–1960.

Phillips, B.L., Brown, G.P., Webb, J.K. & Shine, R. (2006). Invasion and the evolution of speed in toads. *Nature*, 439, 803–803.

R Core Team (2020). *R: A language and environment for statistical computing*. R Foundation for Statistical Computing, Vienna, Austria.

Shaw, A.K., Lutscher, F. & Popovic, L. (2023). Pushed to the edge: Spatial sorting can slow down invasions. *Ecol. Lett.*, 26, 1293–1300.

Skellam, J.G. (1951). Random Dispersal in Theoretical Populations. *Biometrika*, 38, 196–218.

Slatyer, R.A., Hirst, M. & Sexton, J.P. (2013). Niche breadth predicts geographical range size: A general ecological pattern. *Ecol. Lett.*, 16, 1104–1114.

Szűcs, M., Vahsen, M.L., Melbourne, B.A., Hoover, C., Weiss-Lehman, C. & Hufbauer, R.A. (2017). Rapid adaptive evolution in novel environments acts as an architect of population range expansion. *Proc. Natl. Acad. Sci. U.S.A.*, 114, 13501–13506.

Urquhart-Cronish, M., Angert, A.L., Otto, S.P. & MacPherson, A. (2022). Density-dependent selection during range expansion affects expansion load in life-history traits. *bioRxiv*, 2022.11.08.515702.

Viechtbauer, W. (2010). Conducting meta-analyses in R with the metafor package. *J. Stat. Softw.*, 3, 1–48.

Volkova, P.A., Nachatoi, V.A. & Bobrov, A.A. (2023). Hybrid between *Lemna minor* and *L. turionifera* (*L.* × *japonica*, Lemnaceae) in East Europe is more frequent than parental species and poorly distinguishable from them. *Aquat. Bot.*, 184, 103593.

Wagner, N.K., Ochocki, B.M., Crawford, K.M., Compagnoni, A. & Miller, T.E.X. (2017). Genetic mixture of multiple source populations accelerates invasive range expansion. *J. Anim. Ecol.*, 86, 21–34.

Weiss-Lehman, C., Hufbauer, R.A. & Melbourne, B.A. (2017). Rapid trait evolution drives increased speed and variance in experimental range expansions. *Nat. Commun.*, 8, 14303.

Williams, J.L., Kendall, B.E. & Levine, J.M. (2016). Rapid evolution accelerates plant population spread in fragmented experimental landscapes. *Science*, 353, 482–485.

Williams, J.L., Hufbauer, R.A. & Miller, T.E.X. (2019). How evolution modifies the variability of range expansion. *Trends Ecol. Evol.*, 34, 903–913.

Zilio, G., Krenek, S., Gougat-Barbera, C., Fronhofer, E.A. & Kaltz, O. (2023). Predicting evolution in experimental range expansions of an aquatic model system. *Evol. Lett.*, 7, 121–131.

597

598

599

600

601

602 **Figure legends**

603 Figure 1. Experimental range expansion across landscapes with and without a spatial gradient in
604 temperature. (a) Replicate, mixed-genotype populations of *Lemna* expand their experimental
605 ranges across increasingly warmer temperatures (blue to red) from the range core to the range
606 front in gradient landscapes, or across benign and constant temperatures in uniform landscapes.
607 (b) Observed temperatures across gradient (red) and uniform (blue) landscapes during the
608 experiment. Lines represent the slopes of linear models of temperature by distance. We found a
609 significant and positive temperature slope in gradient landscapes ($\beta_{gradient}$ = 0.027, 95% CI:
610 0.027 to 0.028 °C/cm; t = 126.49; P < 0.001) and a slightly negative slope in uniform landscapes
611 ($\beta_{uniform}$ = –0.001, 95% CI: –0.002 to 0.000 °C/cm; t = 68.50; P < 0.01).

612

613 Figure 2. Population dynamics of range expansion across landscapes with (red) and without
614 (blue) a temperature gradient across space. (a) Each line represents the maximum distance
615 travelled over time for a single, replicate range expansion (mean values shown by thick lines).
616 (b) Among-replicate variability (CV) in distance travelled over time for gradient and uniform
617 landscapes. (c) Slope and 95% CI of changes in the log coefficient of variation ratio (lnCVR)
618 over time, where estimates of lnCVR below zero (dashed grey line) indicate that there is less
619 among-replicate variability (CV) across gradient than uniform landscapes. (d-e) Population

620 densities at the range front (i.e., the first 0 to 12 cm) during range expansion. Lines show model
621 predictions from a logistic regression of density across space, with increasing colour intensity
622 representing changes over time from day 4 to 24. (f) Slope and 95% CI obtained from a linear
623 regression of range-front density over time.
624
625 Figure 3. Evolutionary dynamics of range expansion across landscapes with and without a
626 temperature gradient across space. (a) Violin plot for the magnitude of evolution observed in
627 gradient (red) and uniform (blue) landscapes, as quantified as the Euclidean distance of genotype
628 frequencies between founder and evolved populations at the range front. Points show the amount
629 of change in genotype frequencies for each replicate, while dashed lines represent the mean
630 change. (b) Genotype composition of range-front populations in gradient (red) and uniform
631 (blue) landscapes. The first two axes of a Principal Coordinates Analysis (PCoA) are shown,
632 accounting for 43.7% of the total variation in genotype composition. Filled circles are treatment
633 centroids, while clear symbols are replicate populations in each treatment. Ellipses represent one
634 standard deviation around treatment centroids, and lines represent distance from the centroid to
635 each replicate population. (c) Mean genotype frequencies observed across range-front
636 populations in gradient (left) and uniform (right) landscapes, with different colours representing
637 unique genotypes. (d) Genotype frequency for gradient (left) and uniform (right) landscapes.
638 Coloured points and error bars represent observed genotype frequencies and their 95% CIs in
639 evolved range-front populations. The initial genotype frequency in the founder population is
640 denoted by ‘x’.
641

Figure 4. Observed versus simulated among-replicate variability in range-front genotype composition in gradient (top) and uniform (bottom) landscapes. Histograms represent the predicted probability distribution of among-replicate variability in genotype composition due to random sampling alone, with black dotted lines representing the 95% confidence interval. Vertical dashed red and blue lines represent the mean observed among-replicate variability in genotype composition for gradient and uniform landscapes, respectively. Among-replicate variability in genotype composition was quantified as the summed Euclidean distance between the genotypic composition of each replicate population and the mean genotypic composition of each treatment.

Figure 1

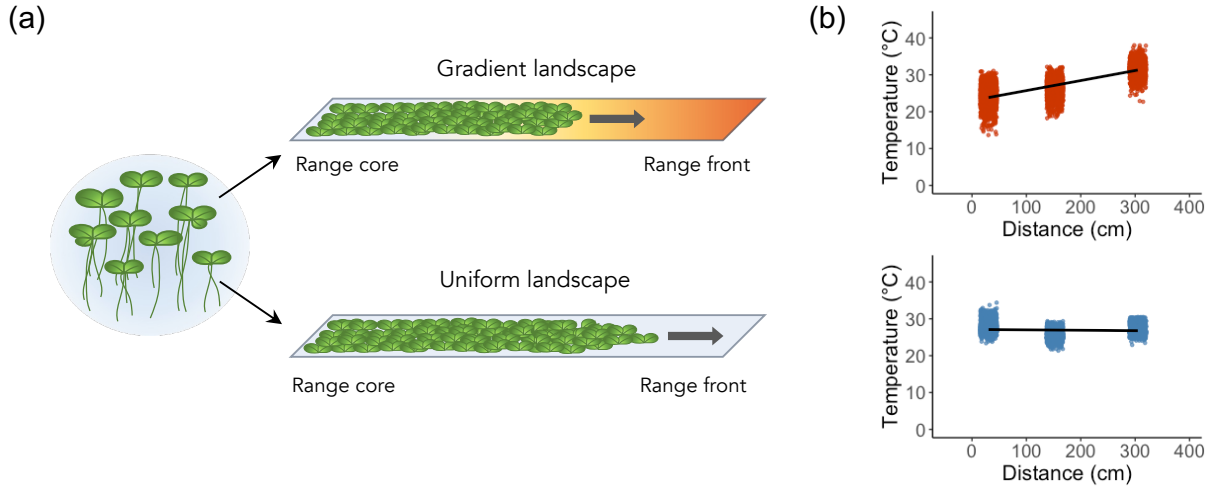
(a)
Gradient landscape
Range core
Range front
Uniform landscape
Range core
Range front
(b)
Temperature (°C)
Distance (cm)
Temperature (°C)
Distance (cm)

673 **Figure 2**

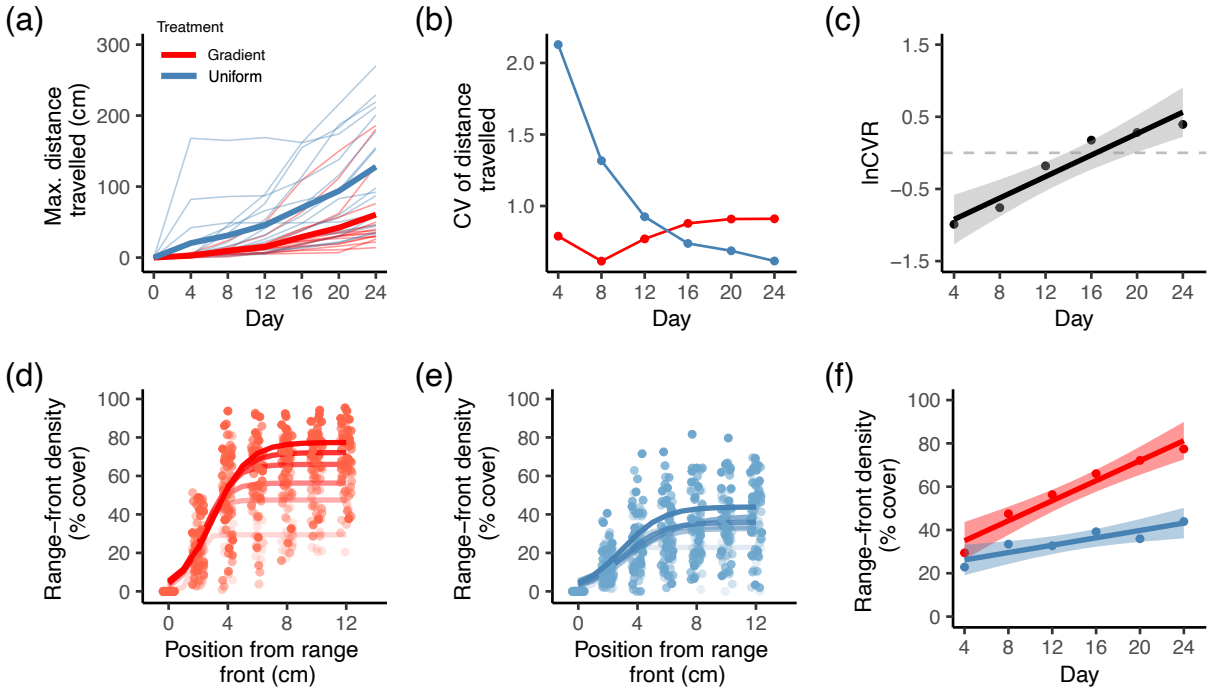

674

675

676

677

Figure 3

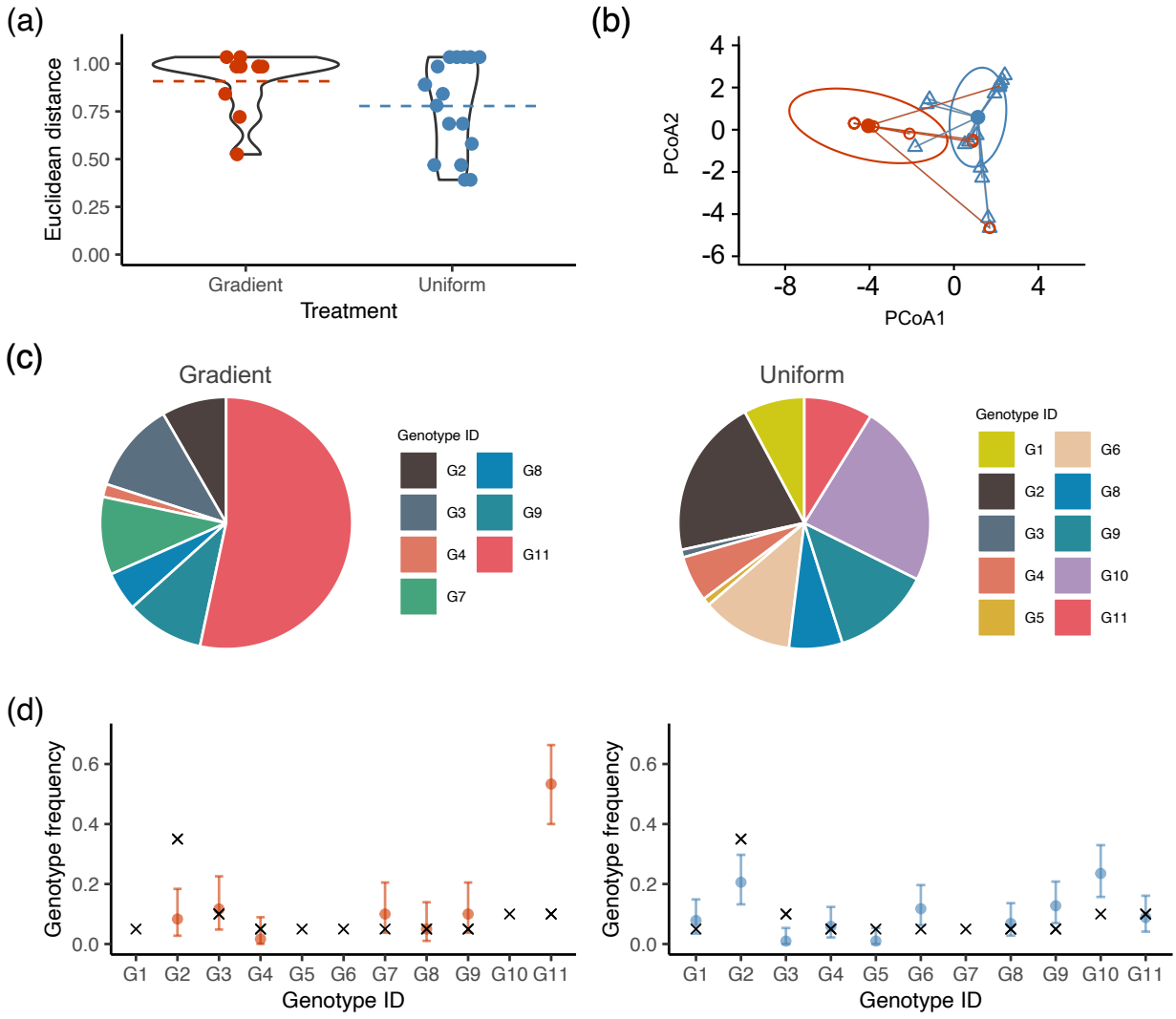
(a)
Euclidean distance
1.00
0.75
0.50
0.25
0.00
Gradient
Uniform
Treatment
(b)
PCoA2
4
2
0
-2
-4
-6
-8
-4
0
4
PCoA1
(c)
Gradient
Genotype ID
G2
G3
G4
G7
G8
G9
G11
Uniform
Genotype ID
G1
G2
G3
G4
G5
G6
G8
G9
G10
G11
(d)
Genotype frequency
0.6
0.4
0.2
0.0
G1 G2 G3 G4 G5 G6 G7 G8 G9 G10 G11
Genotype ID
Genotype frequency
0.6
0.4
0.2
0.0
G1 G2 G3 G4 G5 G6 G7 G8 G9 G10 G11
Genotype ID

686 **Figure 4**

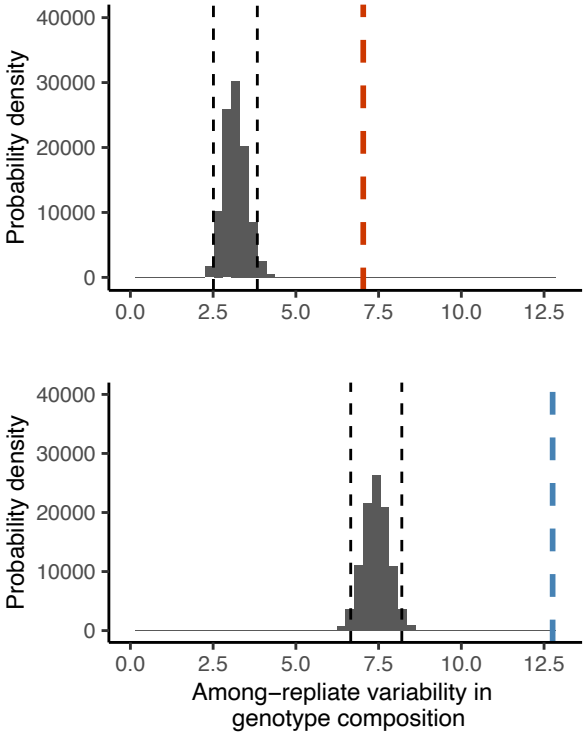

687